Foraging success in planktivorous fish increases with topographic blockage of prey distributions

Johanna M. Aarflot[1,*], Padmini Dalpadado[2], Øyvind Fiksen[3]

[1]Ecosystem Processes Group, Institute of Marine Research, PO Box 1870 Nordnes, 5817 Bergen, Norway
[2]Plankton Group, Institute of Marine Research, PO Box 1870 Nordnes, 5817 Bergen, Norway
[3]Department of Biological Sciences, University of Bergen, PO Box 7803, 5020 Bergen, Norway

ABSTRACT: Banks and shelves are productive zones of the ocean, and often home to large fish stocks. Can shallower bottom topographies improve foraging opportunities for pelagic fish by blocking zooplankton from hiding in deep, darker water? We use mechanistic principles of visual prey search and an extensive dataset of zooplankton depth distributions to model foraging success in planktivorous fish across a large marine ecosystem. Our results show that zooplankton distribute deeper with deeper bathymetry, and that fish find exponentially less food with increasing bottom depths. Over shallow banks, zooplankton are forced into higher light exposure, providing higher prey encounter rates for fish despite lower abundance of prey. Stomach data analyses from a key planktivore support these predictions and suggest that fish foraging on copepods are more successful over shallower grounds. Our study demonstrates that prey availability for planktivorous fish is not proportional to zooplankton abundance, while the bottom depth is an important factor in fish foraging success and zooplankton mortality rates.

KEY WORDS: Bathymetry · Predator–prey interaction · Calanus · Capelin · Seascape ecology · Continental shelf · Barents Sea

1. INTRODUCTION

Banks and shelves in the ocean are often associated with abundant fish communities. Fish aggregation over shallow topographies can be linked to increased food availability, either from enhanced productivity or advection of prey from surrounding areas (Genin 2004, Rogers 2018). Zooplankton over banks and shelves are forced to remain at shallower depths (Isaacs & Schwartzlose 1965, Krumhansl et al. 2018), resulting in increased light exposure, with potential feeding benefits for visual predators (Aarflot et al. 2019). Topographic constraints on zooplankton distribution has been coupled with foraging by planktivores in both marine and freshwater ecosystems (Perissinotto & McQuaid 1992, Fock et al. 2002, Choi et al. 2015), and is presumably important for pelagic fish searching for zooplankton over the seascape.

Consumption of zooplankton by planktivorous fish channels energy from primary production to higher trophic levels and supports important commercial fisheries worldwide (Pikitch et al. 2014, Robinson et al. 2014). Physical and biological factors involved in the predator–prey encounter and feeding process are important drivers of fish stock productivity, biogeography and ecosystem function. For instance, small prey (phytoplankton or microzooplankton) in high prey concentrations or low light levels favor filter feeding, while large, dilute prey favor visual detection and capture of individual prey (Crowder 1985, Batty et al. 1990, van der Lingen 1994).

Light is important for visual foraging. Fish react to prey at greater distances under higher light intensity (Link & Edsall 1996), and water clarity affects both prey choice and consumption (Helenius et al. 2013, Sohel et al. 2017), and the potential for fish production

*Corresponding author: johanna.aarflot@hi.no

(Aksnes 2007). Since light attenuates rapidly with depth in aquatic systems, it is reasonable to expect that deeper prey distributions during daytime reduces fish's ability to locate food. How vertical zooplankton distributions and how topography structure the spatial patterns in visual feeding opportunities for pelagic predators remain, however, poorly understood.

Vertical zooplankton distributions arise from migration strategies related to diel (Bollens & Frost 1991, Ohman & Romagnan 2016) and seasonal (Bandara et al. 2016) cycles, possibly governed by endogenous clock genes (Häfker et al. 2018). Common for these strategies is that they act to optimize individual fitness by balancing the trade-off between growth and survival (Pearre 2003, Ji 2011), and deeper distributions reduce the risk of visual predation (Bandara et al. 2018). Large zooplankton are more easily detected by visual foragers (Aksnes & Giske 1993), and tend to occupy darker parts of the water column (Ohman & Romagnan 2016). Planktivorous fish feed selectively on large prey (Brooks & Dodson 1965), which in addition to greater visibility also contain more energy (Renaud et al. 2018) and support higher growth rates for the fish (van Deurs et al. 2015).

Capelin *Mallotus villosus* is a small pelagic fish with a pivotal role in the northern hemisphere, serving as a key food source for both commercial and non-commercial species (Carscadden et al. 2001, Dolgov 2002). The distribution of capelin is largely associated with continental shelves or shelf seas (Carscadden 2002), and calanoid copepods are a major part of their diet (Astthorsson & Gislason 1997, Dalpadado & Mowbray 2013). The life cycle of calanoid copepods at northern latitudes involve one or more periods of hibernation (Conover 1988), and seasonal vertical migrations transport large amounts of carbon out of the well-lit surface and into deeper waters (Boyd et al. 2019). Our study area, the Barents Sea, is a sub-Arctic shelf sea that hosts one of the largest stocks of capelin in the world (Eriksen et al. 2017), and where calanoid copepods dominate in mesozooplankton (>200 µm, hereinafter 'zooplankton') biomass (Aarflot et al. 2018). Recent studies from the Barents Sea have shown that vertical zooplankton distributions are constrained by topography, particularly the larger (>2000 µm) sizes which have the deepest distributions (Aarflot et al. 2019).

We hypothesize that the bathymetry structures foraging opportunities for pelagic, planktivorous fish in the Barents Sea, as ambient light becomes increasingly limiting for visual foraging when zooplankton are distributed deeper in the water column. Topographic constraints on zooplankton depth distribu-tions should enhance the likelihood of prey detection for fish over shallow topographies. To evaluate these hypotheses, we use an extensive dataset (594 sampling stations) on size-structured, vertical zooplankton distributions as input to a mechanistic foraging model parameterized for a capelin-like fish. Combining the vertical zooplankton data and the foraging model, we can quantify and integrate the prey encounter rate for fish over the water column. We analyze data of copepods in 7597 capelin stomachs collected during multiple surveys, for comparison with our theoretical predictions. Our aim is to assess how bathymetry structures the foraging potential for pelagic fish searching for zooplankton over deep troughs and shallow banks in the Barents Sea(scape).

2. MATERIALS AND METHODS

2.1. Zooplankton data

Data on vertical zooplankton distributions were collected with MOCNESS sampling gear (Wiebe et al. 1985) during autumn monitoring surveys between 1992 and 2016 by the Institute of Marine Research (IMR), Norway. The MOCNESS has a 1 m² opening, 180 µm mesh size, and samples zooplankton in up to 8 depth strata in the water column. Standard depths for MOCNESS sampling in the Barents Sea cover the strata 0–25, 25–50, 50–100, 100–150, 150–200, 200–300, 300–400 and 400–500 m, though there are deviations from this in the data linked to the local bathymetry and associated number of nets deployed per sampling station. The mean distance to the sea floor in our data was 20 m. We restricted our dataset to samples covering >75% of the water column and collected in the daytime, when fish can detect prey by vision. Samples were sorted as day/night based on hour and latitude at the onset of sampling, using an algorithm from the HYbrid Coordinate Ocean Model (HYCOM) (Bleck 2002) and assuming surface irradiance >1 µmol m^{-2} s^{-1} for daytime samples. From our dataset, 9 stations were removed due to missing values in >1 depth strata, in addition to 1 extreme datapoint considered an outlier, leaving 594 stations with vertical zooplankton distributions for our analyses. The data were sampled between day of the year 214 and 280 (early August to early October).

Samples were routinely filtered into 3 size fractions using mesh gauzes of 2000, 1000 and 180 µm, and the data measured as dry weight (g dw m^{-3}). We focused only on the medium (1000–2000 µm, M) and large (>2000 µm, L) size fractions here, assuming these

constitute the most important prey items for capelin (Huse & Toresen 1996, McNicholl et al. 2016). Macrozooplankton in the large size fraction are routinely sorted out (by visual screening) before drying and weighed separately by taxonomic group. For euphausiids, this routine has been in place over the whole data series considered here, while larger amphipods and chaetognaths have been measured separately only since 2008 and may thus be part of the large size fraction in samples from before 2008. However, we expect macrozooplankton to be underrepresented in these samples due to their swimming and net-avoidance capabilities and the sampling gear mesh size (Wiebe et al. 1982, Skjoldal et al. 2013).

Biomass in the upper and lower sampling strata were extrapolated to the surface and bottom, respectively, and we converted biomass to abundance data using a fixed individual dry weight for each size fraction (Table A1 in the Appendix). Calanoid copepods dominate the zooplankton biomass in the Barents Sea (Aarflot et al. 2018), and we used characteristics from 2 *Calanus* species of different sizes (*C. finmarchicus* and *C. hyperboreus*) to represent the 2 size fractions analyzed (M and L, respectively). In the

case of missing biomass values in a depth stratum (14 strata in total, samples lost e.g. due to bad weather conditions), we interpolated between the depth strata. The weighted mean depth (e.g. Dupont & Aksnes 2012) for each size fraction was used as a measure of how deep the copepods were distributed in the water column (Eq. 1 in Table 1).

2.2. Modeling prey encounter rates for fish

We employed a theoretical model of visual foraging (Aksnes & Utne 1997) to approximate prey encounter rates for fish from the observed, vertical zooplankton distributions (Eqs. 2–7 in Table 1, parameters in Table A1). A similar modeling framework has previously been employed to investigate how fish abundance and zooplankton body size varies between fjord systems with different water clarity (Aksnes et al. 2004), seasonality in fish growth in relation to prey abundance and solar irradiance (Varpe & Fiksen 2010), and the relationship between prey size and growth of planktivorous fish (van Deurs et al. 2015).

Table 1. Equations used for estimating weighted mean depth of vertical zooplankton distributions (Eq. 1), prey encounter potential for visual feeding fish (Eqs. 2–7) and estimating the partial fullness index (*PFI*) of copepods in capelin stomachs (Eq. 8). Values and references for constant parameters (*C*, *A*, *s*, *V*, *k* and I_0) are provided in Table A1 in the Appendix. dw: dry weight; *L*: large size fraction; *M*: medium size fraction

Eq.	Description (units)	Equation	Parameters and explanations
1	Zooplankton weighted mean depth[a] (m)	$WMD_j = \sum_{i=1}^{n} \dfrac{\Delta Z_i Z_{m,i} b_{j,i}}{B_j}$	*i*: sampling stratum; Z_i: stratum thickness; $Z_{m,i}$: stratum mean depth; *n*: number of strata sampled; *j*: zooplankton size fraction (*L*, *M*); $b_{j,i}$: g dw biomass m^{-3} in stratum; B_j: depth-integrated dw (m^{-2})
2	Prey detection distance[b] (m)	$R = \sqrt{C \times A \times s \times \dfrac{I_z}{K_I + I_z}}$	*C*: prey contrast; *A*: prey image area; *s*: eye sensitivity of fish; I_z: ambient irradiance; K_I: fish light satiation; *z*: depth
3	Clearance rate[c] (m^3 s^{-1})	$\beta_{j,z} = \dfrac{1}{2}\pi R_{j,z}^2 V$	*V*: swimming velocity
4	Prey encounter rate[d] (ind. s^{-1})	$e_{j,z} = \beta_{j,z} N_{j,z}$	$N_{j,z}$: prey abundance m^{-3}
5	Integrated encounter rate (prey predator^{-1} m^{-2} s^{-1})	$E_j = \sum_{z=1}^{z=b} e_{j,z}$	*b*: station bottom depth. Note that E_j is expressed as g C m^{-2} s^{-1} in Fig. 2 and Table 2, assuming 50% carbon content of individual body weight
6	Prey availability index	$p_j = \dfrac{E_j}{\sum_{z=1}^{z=b} N_{j,z}}$	Scaled as an index between 0 and 1 by dividing by the maximum p_j
7	Ambient irradiance (µmol m^{-2} s^{-1})	$I_z = I_0 \exp^{-kz}$	I_0: surface irradiance; *k*: diffuse attenuation coefficient
8	Capelin stomach fullness (partial fullness index)[e]	$PFI = \dfrac{c}{l^3} \times 10^4$	*c*: g dw of copepods in stomach; *l*: fish length in cm

[a]E.g. Dupont & Aksnes (2012); [b]Approximation by Aksnes & Utne (1997); [c]E.g. Varpe & Fiksen (2010); [d]Holling (1966); [e]Lilly & Fleming (1981), Dalpadado & Mowbray (2013)

Prey encounter rates were estimated as the product of the volume searched by a single fish (m^3 s^{-1}) and prey abundance from the vertical zooplankton data (ind. m^{-3}) (Holling 1966). Similar to Varpe & Fiksen (2010), we modeled the search rate as a function of the fish's swimming velocity (V, m s^{-1}) and prey detection distance (R), assuming only half of the visual field is efficiently scanned for prey e.g. due to overlapping search fields in schools (Eggers 1976). For simplicity, we used the approximation for R which is valid for small prey sizes or low turbidity (Aksnes & Utne 1997, Huse & Fiksen 2010) (our Table 1).

Light attenuation affects how deep surface irradiance penetrates the water column, and the detection distance is sensitive to the diffuse attenuation coefficient k (Fig. 1A). Prey size also affects the detection distance, and longer R for large prey supports higher encounter rates for fish at similar densities of prey (Fig. 1B). When light becomes limiting for prey detection, either due to deep prey distributions or reduced water clarity (or both), the encounter rate decreases. Then, maximum encounter rates peak closer to the surface even if maximum prey density is deeper in the water column (Fig. 1B).

By integrating the estimated encounter rates over the water column (E_j, Table 1), we get a measure of the foraging potential for fish per m^2 area given the size-structured vertical distribution of zooplankton in the water column below. The quotient of the integrated encounter rate and the integrated prey abundance (scaled between 0 and 1) provides an index of prey availability (p_j, Table 1), i.e. how much of the existing prey per m^2 area the fish can detect by vision. A high value indicates that fish can utilize (visually detect) a large fraction of the available prey population because more prey occupies water masses with adequate light for detection. A low value indicates that fish are less able to utilize the measured prey population, as a larger fraction of the prey are found deeper where detection is limited by ambient light. Inversely, a low value also indicates a low predation rate on zooplankton from fish.

2.3. Capelin stomach data

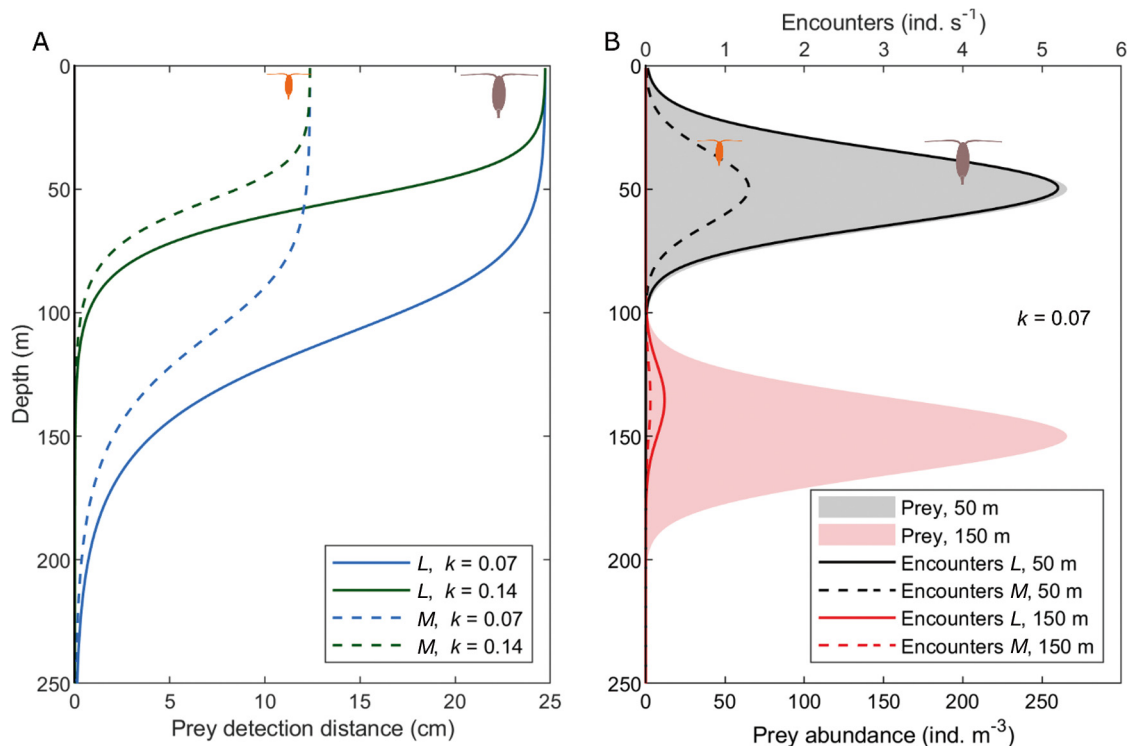To test our hypothesis that the bathymetry affects capelin foraging efficiency, we also analyzed data on

Fig. 1. Modeled (A) prey detection distance and (B) prey encounter rate for a 14 cm planktivorous fish searching for large (L, 5 mm) and medium (M, 2.5 mm) zooplankton prey. Detection distances in (A) (R, Table 1) are shown for 2 levels of water column light absorption (diffuse attenuation coefficient, k). Clear water in the Barents Sea is typically characterized by k around 0.07 (m^{-1}) (Sakshaug et al. 2009). Filled areas in (B) show prey abundance normally distributed around 50 and 150 m

copepods in capelin stomachs. Copepods are the prey group best represented by the MOCNESS data utilized in the foraging model, and the most important prey for capelin apart from euphausiids (Huse & Toresen 1996, Dalpadado & Mowbray 2013). Capelin stomachs were sampled during the same ecosystem monitoring surveys as the zooplankton data between 2005 and 2016, in a joint effort between the IMR and the Knipovich Polar Research Institute of Marine Fisheries and Oceanography (PINRO) (Eriksen et al. 2018). A detailed description of the sampling procedures is given in Dalpadado & Mowbray (2013). Briefly, capelin were sampled with pelagic or bottom trawls, and the stomachs of 10 random individuals per station were analyzed for prey content. The content of copepods in fish stomachs was expressed as a Partial Fullness Index (PFI) (Lilly & Fleming 1981, Dalpadado & Mowbray 2013), which is a function of fish length (Table 1) and hence allows for comparison of prey quantity in stomachs from predators of various sizes.

Analyses on capelin stomachs comprised data from 7597 individual capelin caught between August 4 and October 2. Note that although capelin stomachs and vertical zooplankton data originate from the same monitoring surveys, they are not directly comparable since they were collected at different sampling locations over the years. Accounting for non-linear relationships in the stomach data, we employed generalized additive models (GAMs) using the mgcv package (Wood 2017) in R (version 3.5.0; R Core Team 2018) to evaluate the stomach filling of capelin as a function of bottom depth. A large part (59%) of the stomachs analyzed did not contain copepods, so we fitted 2 types of models: (1) binomially distributed GAMs of presence/absence of copepods in stomachs, and (2) Gaussian distributed GAMs of ($\log_e$) PFI in stomachs with presence of copepods. Longitude/latitude were included as predictors to account for spatial variation in the data, and we tested whether the smoothers for depth varied with the gear type (demersal or pelagic trawl) used to catch capelin. We also tested 3-way interaction models allowing the smoother for depth to differ with gear type and day/night as defined in Section 2.1 above. However, since digestion time may be slow in cold waters (e.g. Bernreuther et al. 2009, Fall & Fiksen 2020) and considering that our definition of day- and nighttime does not include irradiance sources that may generate light other than solar illumination (e.g. Last et al. 2016), we focus on models without a day/night effect.

3. RESULTS

The predicted amount of food available to fish was poorly explained by zooplankton abundance (biomass m^{-2}) over the seascape (Fig. 2A–D). Large zooplankton (L) had no particular geographical trend in biomass (Fig. 2A), yet we estimated the highest prey encounter rates from samples collected at or in close association with banks ≤200 m deep (dark points in Fig. 2C). Non-parametric Mann-Whitney U-tests confirmed that areas shallower than 200 m had higher encounter rates of large prey compared to deeper regions (p < 0.0001, Table 2), even though large zooplankton were more abundant in the deeper areas (p < 0.0001, Table 2). Stations where large zooplankton had a weighted mean depth (WMD_L, Table 1) shallower than 200 m scored high in terms of prey availability, and the prey availability index decreased exponentially with deepening prey distributions (Fig. 2E). Large zooplankton have deeper distributions in deeper regions of the Barents Sea (see e.g. vertical profiles visualized in Aarflot et al. 2019). Consequently, fish can detect a larger part of the zooplankton population in shallow areas (Fig. 2C,E, Table 2).

Medium-sized zooplankton (M) was the dominant prey category in our dataset (Fig. 2B), with a mean of 5.63 g dw m^{-2}, compared to 1.65 g dw m^{-2} for the large size fraction. This converts to abundances of 22520 and 916 ind. m^{-2}, assuming a dry weight content of 250 and 1800 µg ind.$^{-1}$, respectively (Table A1). Despite differences in abundance, the M and L prey groups were comparable in terms of predicted grams of carbon encounter potential for the fish (Fig. 2C–F), with the exception of high mean encounter rates on large zooplankton in shallow areas (Table 2). We estimated high encounter rates on medium-sized prey from samples collected in both shallow and deep areas (dark points in Fig. 2D). However, despite more biomass in deeper areas, there was no difference in prey encounter rates between deep and shallow areas for the medium size class (p = 0.948, Table 2). As with the large size fraction, we found that prey availability for fish decreased with deepening distributions (WMD_M) of the medium-sized zooplankton (Fig. 2F).

Capelin stomachs with the highest copepod content were mainly associated with banks in the central and northern parts of the Barents Sea (Fig. 3A), in accordance with the predicted spatial pattern of prey encounter potential for fish searching for large zooplankton (Fig. 2C). The GAMs (Table 1) further supported our expectation that a shallow bottom depth supports capelin foraging on copepods in the Barents
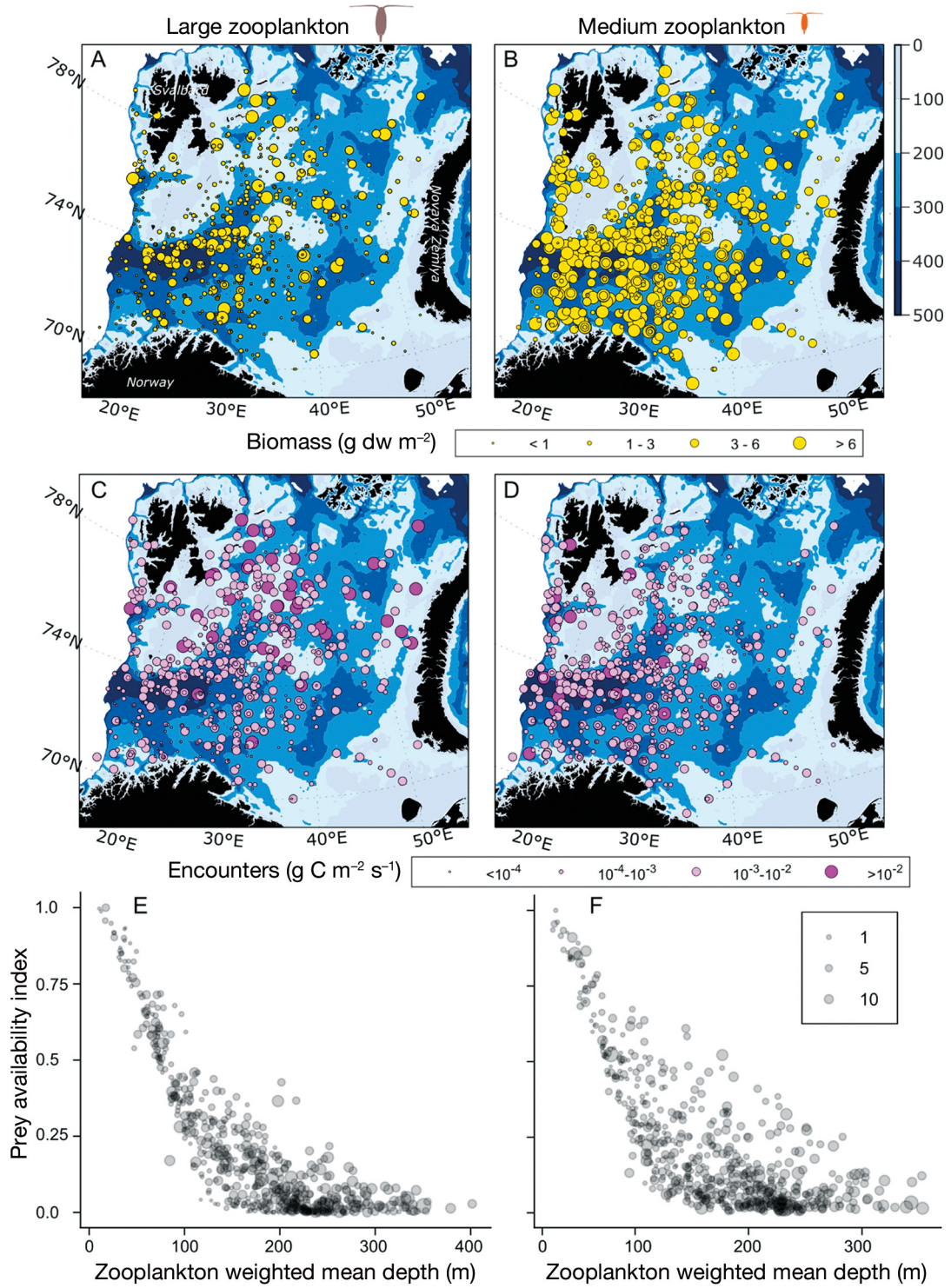
Fig. 2. Fish foraging opportunities on (A,C,E) large (>2000 μm) and (B,D,F) medium-sized (1000–2000 μm) zooplankton. (A,B) Zooplankton biomass, and (C,D) the modeled prey encounter rates for fish based on the vertical depth profiles in (A,B). Bathymetry from the ETOPO database is plotted with light colors for areas ≤ 200 m depth, and darker blue for deeper areas (color key in panel B). (E,F) Prey availability index in relation to the zooplankton weighted mean depth; this index is a function of C/A and D/B (see Eq. 6 in Table 1). Points in (E,F) are plotted with transparency (dark areas = multiple points), and point sizes are proportional to prey biomass (g dw m^{-2}, see size key in panel F). Zooplankton data restricted to samples collected during daytime (n = 594; pooled for years 1992–2016). dw: dry weight

Table 2. Summary of zooplankton biomass and estimated prey encounter rates for planktivorous fish in deep (n = 457) and shallow (n = 137) regions of the Barents Sea. Encounter rates converted to grams of carbon (g C) by assuming 50% carbon content of individual body weight. See also boxplots in Fig. A1 in the Appendix. *Significant difference between deep and shallow areas, p < 0.0001 (2-sided, non-parametric Mann-Whitney *U*-test)

Zooplankton	Measure		Deep (>200 m)	Shallow (≤200 m)
Large (*L*)	Biomass* (g dw m^{-2})	Mean	1.8	1.15
		Median	1.19	0.54
		SEM	0.09	0.12
	Encounters* (E_L, 10^{-3} g C m^{-2} s^{-1})	Mean	2.2	4.84
		Median	0.81	2.08
		SEM	0.16	0.54
Medium (*M*)	Biomass* (g dw m^{-2})	Mean	5.97	3.31
		Median	4.79	1.79
		SEM	0.24	0.35
	Encounters (E_M, 10^{-3} g C m^{-2} s^{-1})	Mean	2.47	2.1
		Median	0.97	1.22
		SEM	0.22	0.24

Sea. Depth had a positive effect on the probability of copepods in capelin stomachs for both gear types in areas between 100 and 200 m, after which it declined (Fig. 3B, p < 0.0001, Table 3). Stomach fullness ($\log_e(PFI)$) also peaked in areas ≤200 m for both gear types (Fig. 3B, p < 0.0001, Table 3). These results did not change with the 3-way interaction models (i.e. including day/night separation of the data), which showed largely quantitative and not qualitative differences (results not shown).

4. DISCUSSION

Predator–prey dynamics in the pelagic habitat are rarely considered in relation to the bottom topography, but here we show that the distance from the surface to the sea floor can have a major effect on fish foraging opportunities and zooplankton mortality risk. Fish can utilize a larger part of the zooplankton standing stock in shallow waters with more light (*WMD* < 200 m, Fig. 2E,F). When distributions are deeper, light becomes limiting for zooplankton detection and they are less available to planktivores (Kaartvedt 1996). Here, we used an extensive dataset on vertical zooplankton distributions and mechanistic principles of visual foraging to model the effect of topography on fish foraging opportunities per m^2 area, which revealed spatial patterns with depth over the seascape. We predicted that banks (≤200 m depth) are zones of relatively high predation rates for fish searching for large zooplankton. We also found that capelin were more successful feeding on copepods over banks compared to deeper areas, supporting this prediction.

Vertical zooplankton distributions can be constrained for several reasons. Diel vertical migrators

Table 3. Model output from generalized additive models assessing presence/absence and partial fullness index ($\log_e(PFI)$) of copepods in capelin stomachs (n = 7597) as a smooth function (s) of bottom depth estimated separately (by) for each trawl type (gear, 'pelagic' or 'demersal'). Geographical position (latitude, longitude) was included in the models to account for spatial variation in the data. Smoothers for covariates Depth and Lat,Lon were restricted to 5 and 20 degrees of freedom, respectively. edf: estimated degrees of freedom

|	Presence/absence model: PAcopepods = gear + s(depth, by = gear) + s(lat,lon)				Presence model: $\log_e(PFI)$ = gear + s(depth, by = gear) + s(lat,lon)			
	Family	Link		Deviance explained (%)	Family	Link		Deviance explained (%)
	Binomial	Logit		13.4	Gaussian	Identity		15
Intercepts	Estimate	SE	*Z*	p	Estimate	SE	*Z*	p
Demersal	−0.713	0.04	−17.23	<0.0001	−3.581	0.06	−63.05	<0.0001
Pelagic	−0.057	0.06	11.75	<0.0001	0.383	0.07	5.298	<0.0001
Smoothers	Levels	edf	χ^2	p	Levels	edf	*F*	p
Depth (by)	Demersal	3.595	317.72	<0.0001	Demersal	3.786	33.88	<0.0001
	Pelagic	3.571	59.33	<0.0001	Pelagic	3.433	8.96	<0.0001
Lat,Lon		17.611	334.92	<0.0001		17.151	14.55	<0.0001
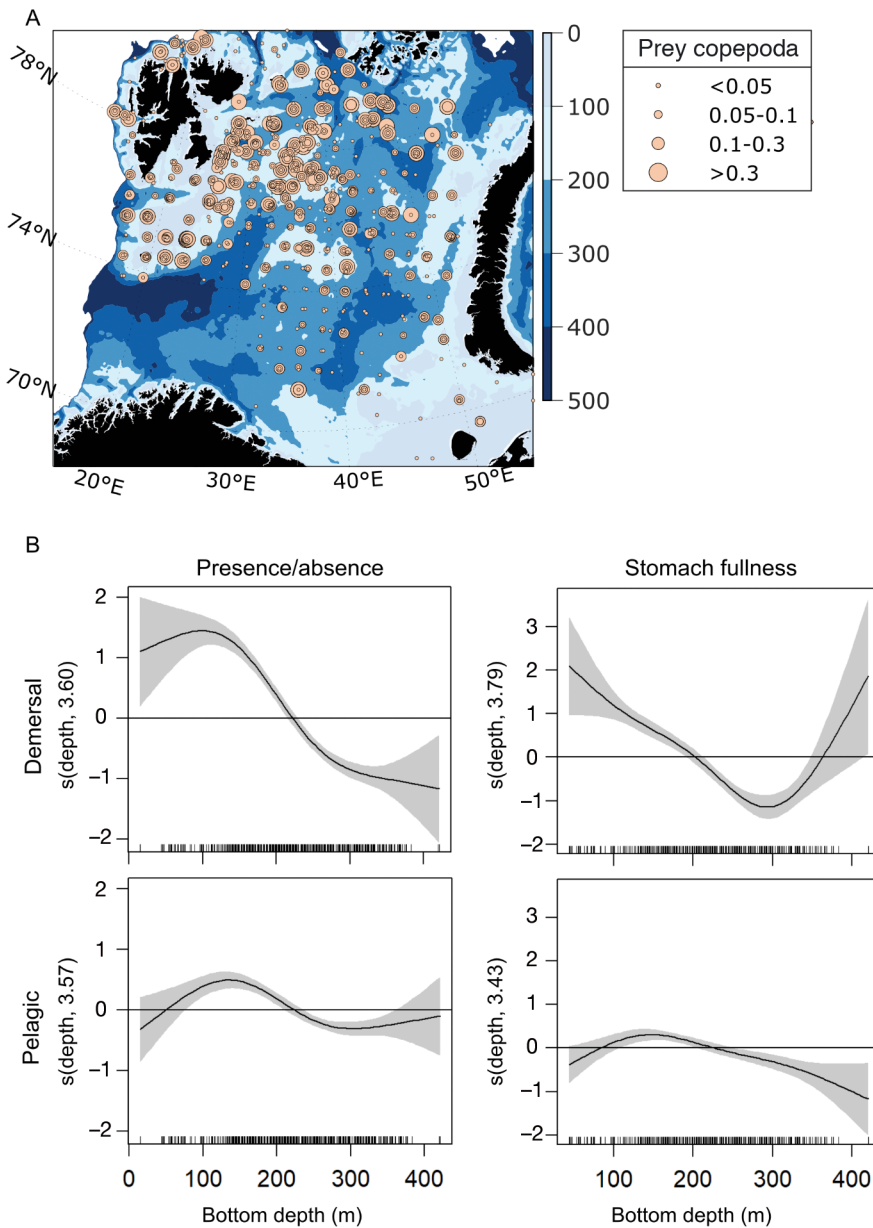
Fig. 3. Effect of bottom depth on stomach filling of prey group Copepoda in capelin (n = 7597; pooled for years 2005–2016). (A) Geographical distribution of the partial fullness index (*PFI*, Table 1), with bathymetry plotted using light colors for areas ≤200 m depth and darker blue for deeper regions. (B) Partial effect of bottom depth on the probability (presence/absence) of copepods in capelin stomachs, and the fullness of copepods ($\log_e(PFI)$) in stomachs where copepods were present, and the effect is shown by trawl type (pelagic or demersal) used to sample capelin. Grey bands correspond to ±2 SE of the estimated generalized additive model smoothers (s, edf values from Table 3 are shown), and rug plots along the *x*-axes correspond to observations along the range of the covariate. Horizontal lines: zero effect

(DVM) may be advected onto shallow coastal regions when occupying surface waters at night, and become trapped by the bathymetry in their descent to deeper waters when daylight returns (Isaacs & Schwartzlose 1965). Similarly, this mechanism may apply to oceanic DVM zooplankton advected onto seamounts (Seki & Somerton 1994, Haury et al. 2000, Rogers 2018), shelf breaks (Robinson & Gómez-Gutiérrez 1998) and banks (Genin et al. 1994). Zooplankton can also become constrained by the bathymetry when seasonally descending for overwintering. *Calanus* species in high-latitude, northern ecosystems descend to overwintering habitats between 500 and

1000 m or deeper in oceanic regions (Østvedt 1955, Hirche 1991), and the bathymetry constrains deep migrations in shelf systems both in the Northwest (Krumhansl et al. 2018) and Northeast (Aarflot et al. 2019) Atlantic. Oxygen concentration is another type of environmental barrier which may limit vertical distributions (Sakwińska & Dawidowicz 2005, Gilly et al. 2013), depending on species' tolerance for hypoxia.

Barriers to vertical distribution may be important for predators searching for pelagic prey. Bathymetric constraints on DVM prey have been suggested to supply demersal fish (Isaacs & Schwartzlose 1965, Genin et al. 1994), seabirds (Hunt et al. 1996) and
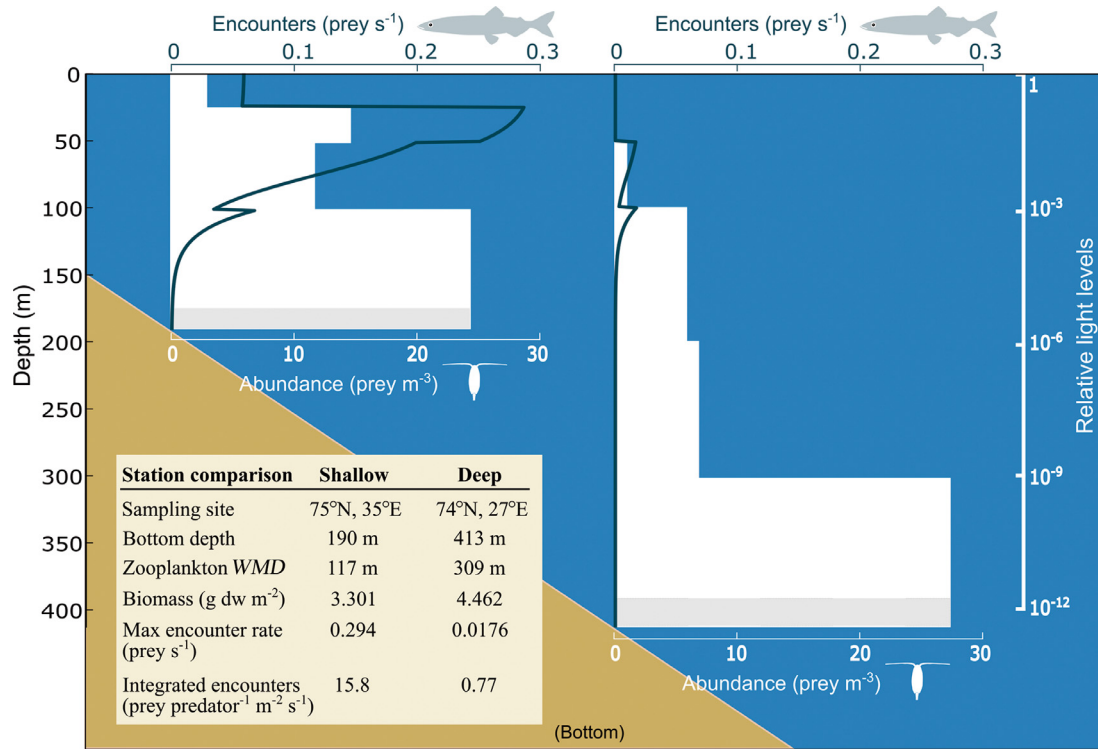
Fig. 4. Zooplankton vertical distributions (white bars) and modeled prey encounter rates for fish (dark blue line) at a shallow (left graph) and deep (right graph) sampling site in the Barents Sea. Shaded grey areas illustrate extrapolated zooplankton abundance (lowest sampling depth to bottom). The bottom topography (brown area) forces zooplankton to remain at relative light levels orders of magnitude higher at the shallow compared to the deep station. This has a large effect on foraging opportunities for a fish stock, with integrated prey encounters differing by a factor of 20 between the 2 sites. dw: dry weight; *WMD*: weighted mean depth

penguins (Perissinotto & McQuaid 1992) foraging over shallow topographies. Similarly, shallow oxygen minimum zones may benefit predators of vertically migrating mesopelagic fish (Stewart et al. 2018).

Light and optical properties of water can structure marine ecosystems. In a comparison of Norwegian fjords with differences in water clarity, Aksnes et al. (2004) found that planktivorous fish abundance was proportional to the size of the integrated visual feeding habitat, and the optical properties of water can shift the competitive balance between fish and jellies (Aksnes et al. 2009, Haraldsson et al. 2012). The relative exposure of zooplankton populations to light in shallow compared to deeper areas may differ by several orders of magnitude (Fig. 4, this study; Aarflot et al. 2019), and ambient light has a major effect on fish visual range (Fig. 1A), which furthermore is squared to get potential search volume for the fish (Table 1).

Does bottom topography also affect ecosystem structure and dynamics because of the local effects on fish foraging efficiency? We discuss this question using 2 randomly chosen stations in our dataset, 1 shallow (190 m) and 1 deep (413 m), with similar zooplankton biomass m^{-2}. The integrated prey encounter rates in the 2 vertical zooplankton profiles differ by a factor of about 20 (Fig. 4). From the results in Aksnes et al. (2004), we would expect the shallower station to support more fish production compared to the deeper one. Zooplankton, on the other hand, have higher survival in regions where the bathymetry allows deeper distributions (low prey availability index, Fig. 2E,F). Survival through the winter could ensure an earlier start of the growth season, and supply fish larvae and juveniles with food in the form of nauplii and small copepodites (e.g. Pedersen & Fossheim 2008).

We propose that topographic blockage of zooplankton increases fish production in areas where fish can utilize this lipid-rich resource even after they descend for overwintering. In the neighboring Norwegian Sea, copepods can descend to 1000s of meters depth to overwinter and become unavailable to pelagic fish. Continental shelves with a varied bathymetry such as the Barents Sea contain important structures both for fish foraging and for zooplankton survival, a combination of which might be central to the high production of fish in this ecosystem (e.g. Hunt et al. 2013).

Profitable foraging habitats for fish over shallow topographies depend on advection of prey from the deeper surrounding waters (Isaacs & Schwartzlose 1965, Genin 2004). Without advection, the local prey biomass produced over these topographies may become depleted. The depth preference of zooplankton will impact their rate of advection within different water masses, and variability in zooplankton transport may be greater than variation in advection itself (Basedow et al. 2018). *C. finmarchicus* is advected with the Atlantic current into the Barents Sea when it ascends to the surface in spring (Skjoldal et al. 1992), and modeling studies have suggested that this species would disappear from the Barents Sea after only 4 yr without advection from the core overwintering areas further south (Skaret et al. 2014). Reduced advection of *C. finmarchicus* from the deep Norwegian Sea and into the shallower North Sea has been coupled with weakened growth potential for sandeels *Ammodytes* sp. (van Deurs et al. 2015) and with a reduction in cod (*Gadus morhua*) biomass through the importance of *C. finmarchicus* for cod recruitment (Beaugrand et al. 2003, Beaugrand & Kirby 2010). Advection of energy-rich zooplankton from oceanic waters has also been coupled with the growth of planktivorous fish on continental shelves in the western Pacific (Kooka et al. 2018).

Foraging benefits over shallow bathymetries has a cost. Pelagic fish like capelin are themselves key prey for higher-level predators. Shallow waters provide a larger degree of vertical overlap between pelagic and demersal species, and studies from Newfoundland have demonstrated a negative association between bottom depth and the amount of capelin measured in cod stomachs (Fahrig et al. 1993). Capelin are also important prey for cetaceans which are primarily associated with the banks in the northern Barents Sea (Skern-Mauritzen et al. 2011). Future studies should identify the trade-offs bathymetry creates for migratory and drifting organisms in the ocean, and how marine productivity and trophic interactions change with bathymetry.

Deep and dark prey distributions reduce a fish's foraging efficiency, and vertical descents in zooplankton on both diel and seasonal cycles increase zooplankton survival and fitness (Bollens & Frost 1991, Bandara et al. 2018). Consequently, environmental factors like light attenuation, prey size and bottom depth constraints can be more important than prey abundance for planktivorous fish searching for food in the pelagic realm. Our results point to the possibility that the seascape, or bottom topography and ocean currents in combination, can act as a large-scale zooplankton 'trap' facilitating the production of planktivorous fish in marine ecosystems.

On the other hand, the deep trenches in the Barents Sea provide safe refuges for overwintering copepods, probably adding to the stability and long-term productivity of the system. The spatial heterogeneity and variability of prey vulnerability in the Barents Sea may be understood in light of Huffaker's famous mite experiment (Huffaker 1958), where the deep trenches can be seen as population reservoirs ensuring next-year recruitment and reseeding of the banks with prey.

LITERATURE CITED

Aarflot JM, Skjoldal HR, Dalpadado P, Skern-Mauritzen M (2018) Contribution of *Calanus* species to the mesozooplankton biomass in the Barents Sea. ICES J Mar Sci 75: 2342–2354

Aarflot JM, Aksnes DL, Opdal AF, Skjoldal HR, Fiksen Ø (2019) Caught in broad daylight: topographic constraints of zooplankton depth distributions. Limnol Oceanogr 64: 849–859

Aksnes DL (2007) Evidence for visual constraints in large marine fish stocks. Limnol Oceanogr 52:198–203

Aksnes DL, Giske J (1993) A theoretical model of aquatic visual feeding. Ecol Modell 67:233–250

Aksnes DL, Utne ACW (1997) A revised model of visual range in fish. Sarsia 82:137–147

Aksnes DL, Nejstgaard J, Sædberg E, Sørnes T (2004) Optical control of fish and zooplankton populations. Limnol Oceanogr 49:233–238

Aksnes DL, Dupont N, Staby A, Fiksen Ø, Kaartvedt S, Aure J (2009) Coastal water darkening and implications for mesopelagic regime shifts in Norwegian fjords. Mar Ecol Prog Ser 387:39–49

Astthorsson OS, Gislason A (1997) On the food of capelin in the subarctic waters north of Iceland. Sarsia 82:81–86

Bandara K, Varpe Ø, Søreide JE, Wallenschus J, Berge J, Eiane K (2016) Seasonal vertical strategies in a high-Arctic coastal zooplankton community. Mar Ecol Prog Ser 555:49–64

Bandara K, Varpe Ø, Ji R, Eiane K (2018) A high-resolution modeling study on diel and seasonal vertical migrations of high-latitude copepods. Ecol Modell 368:357–376

Basedow SL, Sundfjord A, von Appen WJ, Halvorsen E, Kwasniewski S, Reigstad M (2018) Seasonal variation in

transport of zooplankton into the Arctic Basin through the Atlantic gateway, Fram Strait. Front Mar Sci 5:194

Batty RS, Blaxter JHS, Richard JM (1990) Light intensity and the feeding behaviour of herring, *Clupea harengus*. Mar Biol 107:383–388

Beaugrand G, Kirby RR (2010) Climate, plankton and cod. Glob Change Biol 16:1268–1280

Beaugrand G, Brander KM, Lindley JA, Souissi S, Reid PC (2003) Plankton effect on cod recruitment in the North Sea. Nature 426:661–664

Bernreuther M, Temming A, Herrmann JP (2009) Effect of temperature on the gastric evacuation in sprat *Sprattus sprattus*. J Fish Biol 75:1525–1541

Bleck R (2002) An oceanic general circulation model framed in hybrid isopycnic-Cartesian coordinates. Ocean Model 4:55–88

Bogstad B, Gjøsæter H (2001) Predation by cod (*Gadus morhua*) on capelin (*Mallotus villosus*) in the Barents Sea: implications for capelin stock assessment. Fish Res 53:197–209

Bollens SM, Frost BW (1991) Diel vertical migration in zooplankton: rapid individual response to predators. J Plankton Res 13:1359–1365

Boyd PW, Claustre H, Levy M, Siegel DA, Weber T (2019) Multi-faceted particle pumps drive carbon sequestration in the ocean. Nature 568:327–335

Brooks JL, Dodson SI (1965) Predation, body size, and composition of plankton. Science 150:28–35

Carscadden J (2002) Capelin — What are they good for? Introduction. ICES J Mar Sci 59:863–869

Carscadden JE, Frank KT, Leggett WC (2001) Ecosystem changes and the effects on capelin (*Mallotus villosus*), a major forage species. Can J Fish Aquat Sci 58:73–85

Choi JY, Jeong KS, La GH, Joo GJ (2015) Spatio-temporal distribution of *Diaphanosoma brachyurum* (Cladocera: Sididae) in freshwater reservoir ecosystems: importance of maximum water depth and macrophyte beds for avoidance of fish predation. J Limnol 74:403–413

Conover RJ (1988) Comparative life histories in the genera *Calanus* and *Neocalanus* in high latitudes of the northern hemisphere. Hydrobiologia 167:127–142

Crowder LB (1985) Optimal foraging and feeding mode shifts in fishes. Environ Biol Fishes 12:57–62

Dalpadado P, Mowbray F (2013) Comparative analysis of feeding ecology of capelin from two shelf ecosystems, off Newfoundland and in the Barents Sea. Prog Oceanogr 114:97–105

Dolgov AV (2002) The role of capelin (*Mallotus villosus*) in the foodweb of the Barents Sea. ICES J Mar Sci 59: 1034–1045

Dupont N, Aksnes DL (2012) Effects of bottom depth and water clarity on the vertical distribution of *Calanus* spp. J Plankton Res 34:263–266

Eggers DM (1976) Theoretical effect of schooling by planktivorous fish predators on rate of prey consumption. J Fish Res Board Can 33:1964–1971

Eriksen E, Skjoldal HR, Gjøsæter H, Primicerio R (2017) Spatial and temporal changes in the Barents Sea pelagic compartment during the recent warming. Prog Oceanogr 151:206–226

Eriksen E, Gjøsæter H, Prozorkevich D, Shamray E and others (2018) From single species surveys towards monitoring of the Barents Sea ecosystem. Prog Oceanogr 166:4–14

Fahrig L, Lilly GR, Miller DS (1993) Predator stomachs as sampling tools for prey distribution: Atlantic cod (*Gadus morhua*) and capelin (*Mallotus villosus*). Can J Fish Aquat Sci 50:1541–1547

Fall J, Fiksen Ø (2020) No room for dessert: a mechanistic model of prey selection in gut-limited predatory fish. Fish Fish 21:63–79

Fock HO, Matthiessen B, Zidowitz H, von Westernhagen H (2002) Diel and habitat-dependent resource utilisation by deep-sea fishes at the Great Meteor seamount: niche overlap and support for the sound scattering layer interception hypothesis. Mar Ecol Prog Ser 244:219–233

Genin A (2004) Bio-physical coupling in the formation of zooplankton and fish aggregations over abrupt topographies. J Mar Syst 50:3–20

Genin A, Greene C, Haury L, Wiebe P and others (1994) Zooplankton patch dynamics: daily gap formation over abrupt topography. Deep Sea Res I 41:941–951

Gilly WF, Beman JM, Litvin SY, Robison BH (2013) Oceanographic and biological effects of shoaling of the oxygen minimum zone. Annu Rev Mar Sci 5:393–420

Häfker NS, Teschke M, Last KS, Pond DW, Hüppe L, Meyer B (2018) *Calanus finmarchicus* seasonal cycle and diapause in relation to gene expression, physiology, and endogenous clocks. Limnol Oceanogr 63:2815–2838

Haraldsson M, Tönnesson K, Tiselius P, Thingstad TF, Aksnes DL (2012) Relationship between fish and jellyfish as a function of eutrophication and water clarity. Mar Ecol Prog Ser 471:73–85

Haury L, Fey C, Newland C, Genin A (2000) Zooplankton distribution around four eastern North Pacific seamounts. Prog Oceanogr 45:69–105

Helenius LK, Borg JPG, Nurminen L, Leskinen E, Lehtonen H (2013) The effects of turbidity on prey consumption and selection of zooplanktivorous *Gasterosteus aculeatus* L. Aquat Ecol 47:349–356

Hirche HJ (1991) Distribution of dominant calanoid copepod species in the Greenland Sea during late fall. Polar Biol 11:351–362

Hirche HJ (1997) Life cycle of the copepod *Calanus hyperboreus* in the Greenland Sea. Mar Biol 128:607–618

Holling CS (1966) The functional response of invertebrate predators to prey density. Mem Entomol Soc Can 98:5–86

Huffaker CB (1958) Experimental studies on predation: dispersion factors and predator-prey oscillations. Hilgardia 27:343–383

Hunt GL Jr, Coyle KO, Hoffman S, Decker MB, Flint EN (1996) Foraging ecology of short-tailed shearwaters near the Pribilof Islands, Bering Sea. Mar Ecol Prog Ser 141:1–11

Hunt GL Jr, Blanchard AL, Boveng P, Dalpadado P and others (2013) The Barents and Chukchi Seas: comparison of two Arctic shelf ecosystems. J Mar Syst 109–110:43–68

Huse G, Fiksen Ø (2010) Modelling encounter rates and distribution of mobile predators and prey. Prog Oceanogr 84:93–104

Huse G, Toresen R (1996) A comparative study of the feeding habits of herring (*Clupea harengus*, Clupeidae, L.) and capelin (*Mallotus villosus*, Osmeridae, Müller) in the Barents Sea. Sarsia 81:143–153

Isaacs JD, Schwartzlose RA (1965) Migrant sound scatterers: interaction with the sea floor. Science 150:1810–1813

Ji R (2011) *Calanus finmarchicus* diapause initiation: new view from traditional life history-based model. Mar Ecol Prog Ser 440:105–114

Kaartvedt S (1996) Habitat preference during overwintering and timing of seasonal vertical migration of *Calanus finmarchicus*. Ophelia 44:145–156

Kooka K, Hamatsu T, Yamamura O (2018) Transported zooplankton from the Okhotsk Sea facilitate feeding and growth of juvenile walleye pollock on a continental shelf along the Oyashio Current, western subarctic Pacific. Mar Biol 165:100

Krumhansl KA, Head EJH, Pepin P, Plourde S, Record NR, Runge JA, Johnson CL (2018) Environmental drivers of vertical distribution in diapausing *Calanus* copepods in the Northwest Atlantic. Prog Oceanogr 162:202–222

Langbehn TJ, Varpe Ø (2017) Sea-ice loss boosts visual search: fish foraging and changing pelagic interactions in polar oceans. Glob Change Biol 23:5318–5330

Last KS, Hobbs L, Berge J, Brierley AS, Cottier F (2016) Moonlight drives ocean-scale mass vertical migration of zooplankton during the Arctic winter. Curr Biol 26: 244–251

Lilly GR, Fleming AH (1981) Size relationships in predation by Atlantic cod, *Gadus morhua*, on capelin, *Mallotus villosus*, and sand lance, *Ammodytes dubius*, in the Newfoundland area. NAFO Sci Counc Stud 1:41–45

Link J, Edsall TA (1996) The effect of light on lake herring (*Coregonus artedi*) reactive volume. Hydrobiologia 332: 131–140

McNicholl DG, Walkusz W, Davoren GK, Majewski AR, Reist JD (2016) Dietary characteristics of co-occurring polar cod (*Boreogadus saida*) and capelin (*Mallotus villosus*) in the Canadian Arctic, Darnley Bay. Polar Biol 39: 1099–1108

Ohman MD, Romagnan JB (2016) Nonlinear effects of body size and optical attenuation on diel vertical migration by zooplankton. Limnol Oceanogr 61:765–770

Østvedt OJ (1955) Zooplankton investigations from weather ship M in the Norwegian Sea, 1948–49. Hvalråd Skr 40: 1–93

Pearre S (2003) Eat and run? The hunger/satiation hypothesis in vertical migration: history, evidence and consequences. Biol Rev Camb Philos Soc 78:1–79

Pedersen T, Fossheim M (2008) Diet of 0-group stages of capelin (*Mallotus villosus*), herring (*Clupea harengus*) and cod (*Gadus morhua*) during spring and summer in the Barents Sea. Mar Biol 153:1037–1046

Perissinotto R, McQuaid CD (1992) Land-based predator impact on vertically migrating zooplankton and micronekton advected to a Southern Ocean archipelago. Mar Ecol Prog Ser 80:15–27

Pikitch EK, Rountos KJ, Essington TE, Santora C and others (2014) The global contribution of forage fish to marine fisheries and ecosystems. Fish Fish 15:43–64

R Core Team (2018) R: a language and environment for statistical computing. R Foundation for Statistical Computing, Vienna

Renaud PE, Daase M, Banas NS, Gabrielsen TM and others (2018) Pelagic food-webs in a changing Arctic: a trait-based perspective suggests a mode of resilience. ICES J Mar Sci 75:1871–1881

Robinson CJ, Gómez-Gutiérrez J (1998) Daily vertical migration of dense deep scattering layers related to the shelf-break area along the northwest coast of Baja California, Mexico. J Plankton Res 20:1679–1697

Robinson K, Ruzicka J, Decker MB, Brodeur R and others (2014) Jellyfish, forage fish, and the world's major fisheries. Oceanography (Wash DC) 27:104–115

Rogers AD (2018) The biology of seamounts: 25 years on. Adv Mar Biol 79:137–224

Sakshaug E, Johnsen G, Volent Z (2009) Light. In: Sakshaug E, Johnsen G, Kovacs K (eds) Ecosystem Barents Sea. Tapir Academic Press, Trondheim, p 117–138

Sakwińska O, Dawidowicz P (2005) Life history strategy and depth selection behavior as alternative antipredator defenses among natural *Daphnia hyalina* populations. Limnol Oceanogr 50:1284–1289

Seki MP, Somerton DA (1994) Feeding ecology and daily ration of the pelagic armorhead, *Pseudopentaceros wheeleri*, at Southeast Hancock Seamount. Environ Biol Fishes 39:73–84

Skaret G, Dalpadado P, Hjøllo SS, Skogen MD, Strand E (2014) *Calanus finmarchicus* abundance, production and population dynamics in the Barents Sea in a future climate. Prog Oceanogr 125:26–39

Skern-Mauritzen M, Johannesen E, Bjørge A, Øien N (2011) Baleen whale distributions and prey associations in the Barents Sea. Mar Ecol Prog Ser 426:289–301

Skjoldal HR, Gjøsæter H, Loeng H (1992) The Barents Sea ecosystem in the 1980s: ocean climate, plankton, and capelin growth. ICES Mar Sci Symp 195:278–290

Skjoldal HR, Wiebe PH, Postel L, Knutsen T, Kaartvedt S, Sameoto DD (2013) Intercomparison of zooplankton (net) sampling systems: results from the ICES/GLOBEC sea-going workshop. Prog Oceanogr 108:1–42

Sohel S, Mattila J, Lindström K (2017) Effects of turbidity on prey choice of three-spined stickleback *Gasterosteus aculeatus*. Mar Ecol Prog Ser 566:159–167

Stewart JD, Barroso A, Butler RH, Munns RJ (2018) Caught at the surface: Myctophids make easy prey for dolphins and devil rays. Ecology 99:1894–1896

Tande KS (1982) Ecological investigations on the zooplankton community of Balsfjorden, northern Norway: generation cycles, and variations in body weight and body content of carbon and nitrogen related to overwintering and reproduction in the copepod *Calanus finmarchicus* (Gunnerus). J Exp Mar Biol Ecol 62:129–142

Utne-Palm AC (1999) The effect of prey mobility, prey contrast, turbidity and spectral composition on the reaction distance of *Gobiusculus flavescens* to its planktonic prey. J Fish Biol 54:1244–1258

van der Lingen CD (1994) Effect of particle size and concentration on the feeding behaviour of adult pilchard *Sardinops sagax*. Mar Ecol Prog Ser 109:1–13

van Deurs M, Jørgensen C, Fiksen Ø (2015) Effects of copepod size on fish growth: a model based on data for North Sea sandeel. Mar Ecol Prog Ser 520:235–243

Varpe Ø, Fiksen Ø (2010) Seasonal plankton-fish interactions: light regime, prey phenology, and herring foraging. Ecology 91:311–318

Wiebe PH, Boyd SH, Davis M, Cox JL (1982) Avoidance of towed nets by the eupahusiid *Nematoscelis megalops*. Fish Bull 80:75–91

Wiebe PH, Morton AW, Bradley AM, Backus RH and others (1985) New development in the MOCNESS, an apparatus for sampling zooplankton and micronekton. Mar Biol 87:313–323

Wood SN (2017) mgcv: mixed GAM computation vehicle with GCV/AIC/REML smoothness estimation. R package. https://cran.r-project.org/package=mgcv

Appendix

Table A1. Parameters employed to model prey encounter potential for planktivorous fish. R: prey detection distance

Model component	Symbol	Description	Value	Unit	Comment (reference)
Fish	BL	Body length	0.14	m	Mature capelin (Bogstad & Gjøsæter 2001)
	V	Swimming velocity	$1.5 \times BL$	m s^{-1}	
	s	Eye sensitivity[a]	$BL^2/(9 \times 10^{-7})$		Scaling as in Langbehn & Varpe (2017)
	K_I	Light satiation (half saturation coefficient for R to I)[a]	1	µmol m^{-2} s^{-1}	
Large copepods (>2000 µm size fraction)	P_l	Prey length	0.005	m	Copepodite stage CV *Calanus hyperboreus* (Hirche 1997)
	P_{wi}	Prey width	$P_l/2$	m	
	P_{dw}	Prey (dry) weight	1800	µg ind.$^{-1}$	Copepodite stage CV *C. hyperboreus* (August) (Hirche 1997)
Medium copepods (1000–2000 µm size fraction)	P_l	Prey length	0.0025	m	Copepodite stage CV
	P_{wi}	Prey width	$P_l/2$	m	*C. finmarchicus* (Tande 1982)
	P_{dw}	Prey (dry) weight	250	µg ind.$^{-1}$	Copepodite stage CV *C. finmarchicus* (Tande 1982)
Copepods[b]	C	Contrast against the background	0.3		*Calanus* spp. (Utne-Palm 1999)
	A	Image area	$P_l \times P_{wi} \times 0.75$[c]	m^2	
Light	I_0	Surface irradiance	200	µmol m^{-2} s^{-1}	
	k	Diffuse attenuation coefficient	0.07	m^{-1}	Clear water Barents Sea (Sakshaug et al. 2009)

[a]Parameters are scaled so that reaction distance $R \sim 1\,BL$ when light is not limiting and prey A is 3×10^{-6} m^2; [b]Same for both sizes; [c]Small, elongated prey
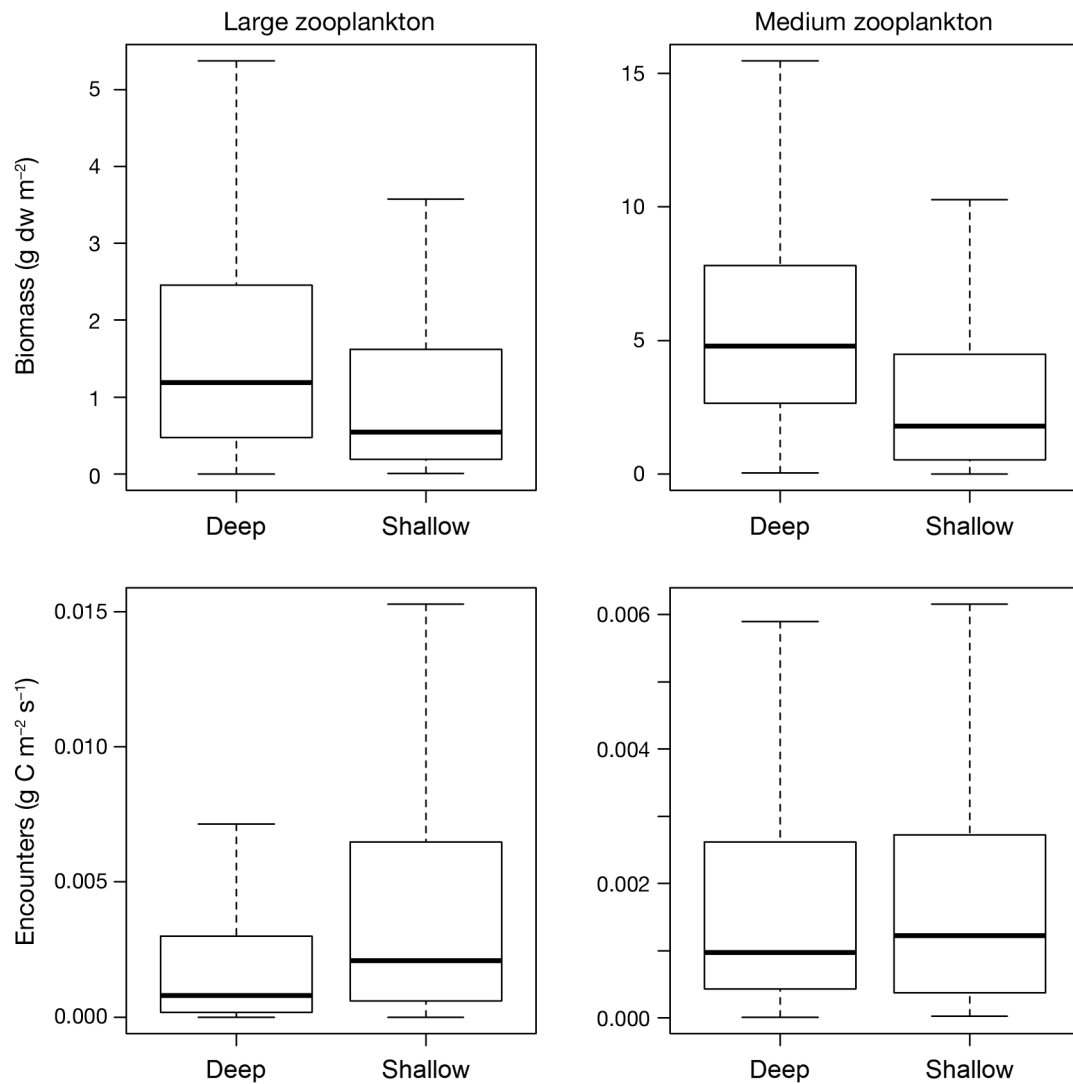
Fig. A1. Distribution of zooplankton biomass (upper panels) and modeled prey encounter rates (lower panels) for planktivorous fish, for large (left panels) and medium (right panels) size zooplankton, in deep (>200 m depth) and shallow (≥200 m depth) regions of the Barents Sea. Boxplots show the median (thick horizontal line in the box), first and third quartiles (lower and upper limits of the box), and whiskers extending to the first 'outlier' in each direction (1.5 × IQR). Datapoints >1.5 × IQR are not shown. Note the different *y*-axis scales